ALGORITHM FOR NON-PROPORTIONAL LOADING IN SEQUENTIALLY LINEAR ANALYSIS

CHENJIE YU [*], P.C.J. HOOGENBOOM [†] AND J.G. ROTS [††]

[*] Delft University of Technology
Delft, the Netherlands
e-mail: Chenjie.Yu@tudelft.nl

[†] Delft University of Technology
Delft, the Netherlands
e-mail: P.C.J.Hoogenboom@tudelft.nl

[††] Delft University of Technology
Delft, the Netherlands
e-mail: J.G.Rots@tudelft.nl

Key words: Concrete, sequentially linear analysis, static non-proportional loading, prestress

Abstract: Sequentially linear analysis (SLA) is an alternative to the Newton-Raphson method for analyzing the nonlinear behavior of reinforced concrete and masonry structures. In this paper SLA is extended to load cases that are applied one after the other, for example first dead load and then wind load. It is shown that every nonlinear analysis step can be made in just two linear elastic analysis steps. The proposed algorithm is extremely robust, which is demonstrated in a prestressed concrete beam analysis. A comparison is made between results of SLA and Newton-Raphson with arch length control.

1 INTRODUCTION

1.1 Background

Nonlinear finite element analysis is becoming a common tool for studying the behavior of reinforced concrete structures. Over the past years, techniques for nonlinear analysis have been enhanced significantly via improved solution procedures, extended finite element techniques and increased robustness of constitutive models. Nevertheless, problems remain, especially when cracking and crushing in real-world structures is analysed. Sequentially linear analysis (SLA) is an alternative to the Newton-Raphson method when bifurcation, snap-back or divergence problems arise. The incremental-iterative procedure, adopted in nonlinear finite element analysis, is replaced by a sequence of scaled linear finite element analyses with decreasing secant stiffness, corresponding to local damage increments. The focus of most research is on reinforced concrete structures, where multiple cracks initiate and compete to survive. Compared to nonlinear smeared crack models in incremental-iterative settings, the sequentially linear model is shown to be robust and effective in predicting localizations, crack spacing and crack width as well as brittle shear behaviour [1].

In static structural analysis, loads are often applied together (proportional loading). However, the load order can be important, for example first prestress on a concrete beam and

subsequently removal of the formwork which activates self-weight. Other examples are pushover loading of a masonry wall with permanent overburden and wind load after snow load on a roof structure. In general, non-proportional loading is the situation that some loads are kept constant while others vary in time.

1.2 Objective

The aim of this study is to extend Sequentially Linear Analysis (SLA) to non-proportional loading. This would enable SLA to be applied to pushover analysis for earthquake loading. The algorithm needs to support general element types and different failure criteria. In addition, the calculation time needs to be minimized.

1.3 Previous research

An initial attempt to implement non-proportional loading for SLA was made by De Jong et al. [2]. Although results were encouraging in that method the stresses may temporarily not satisfy the constitutive equations.

2 IMPLEMENTATION OF NON-PROPORTIONAL LOADING

In proportional SLA the load is the same in every analysis step and scaled by a factor λ, which is determined by the failure criterion for the most critical element. For example, the external load $F_e = \lambda F_u$, where F_u is a unit load. In non-proportional SLA an extra constant load F_c is applied at the same time. The total load is $F_t = \lambda F_u + F_c$. This can be written as $F_t = \lambda(F_u + F_c/\lambda)$. At the beginning of a load cycle λ is unknown, therefore it is estimated by v consequently, $F_t = \lambda(F_u + F_c/v)$. After one linear elastic analysis a better estimate of v can be made $v_2 = \lambda_1$. By repeating this several times v and λ become almost the same and the solution to a load cycle is found. It will be shown that the exact solution can be found in just two linear elastic analyses.

Summarizing, in every load cycle the constant load is divided by a variable v after which the linear elastic analysis is performed and the total load is scaled by a factor λ. Since at the end of each load cycle $v = \lambda$ the dead load remains constant. Below it is explained in detail.

2.1 Non-proportional loading algorithm

Consider a structure with two loads F_c and F_e. The loads are applied one after the other. Load F_c is applied first and kept constant while load F_e is subsequentially added and increased.

1) Apply loads F_c/v_1 and F_u to the structure, replacing the previous loading. v_1 is estimated, for example the previous λ (see 2.6)
2) Perform a linear elastic analysis.
3) Consider all elements and find the largest stress. The load factor λ_1 is basically failure stress over largest stress (see 2.2, 2.3, 2.4).
4) Apply loads F_c/v_2 and F_u to the structure, replacing the previous loading. $v_2 = \lambda_1$.
5) Perform a linear elastic analysis.
6) Consider all elements and find the largest tensile stress. The load factor λ_2 is basically failure stress over "largest" stress.
7) $\lambda_3 = v_3 = \frac{-v_1\lambda_2 v_2 + \lambda_1\lambda_2 v_2 + \lambda_1 v_1 v_2 - \lambda_1 v_1 \lambda_2}{v_1\lambda_2 - \lambda_1 v_2}$ (see 2.6)

Now the situation is that if we multiply the load by λ_3 then the structure is loaded such that the material just fails somewhere and the first load is F_c and the second load is $\lambda_3 F_u$.

8) Reduce the stiffness of the element with the largest stress (see 2.5).
9) If λ is greater than zero then continue at step 1.

2.2 Failure criterion

The failure criterion that has been applied is the Mohr-Coulomb criterion with tension cut-off.

$$\frac{\lambda\sigma_1}{f_{t2}} + \frac{\lambda\sigma_3}{f_{c'}} = 1 \qquad (1)$$

$$\frac{\lambda\sigma_1}{f_t'} = 1 \tag{2}$$

Damaged strengths are used for cutting-off tension f_t' and compression part f_c' (negative value) of the Mohr-Coulomb criterion. (see section 2.3) The tensile strength f_{t2} of the Mohr-Coulomb criterion is constant. It is a fictitious value of two times the normal tensile strength.

2.3 Obtaining the material stiffness

In Ansys APDL the material properties cannot be retrieved directly from element results when running multiple calculations in every step of an analysis. (It is accessible only when the post processor is activated.) However, the stresses and strains can be retrieved directly in every analysis step. Therefore, the stiffness in a principal direction is derived from the principal stresses and strains.

Hooke's law reads

$$\begin{cases} \varepsilon_1 = \frac{\sigma_1}{E_1} - \frac{v_{12}}{E_2}\sigma_2 - \frac{v_{13}}{E_3}\sigma_3 \\ \varepsilon_2 = \frac{-v_{21}}{E_1}\sigma_1 + \frac{\sigma_2}{E_2} - \frac{v_{23}}{E_3}\sigma_3 \\ \varepsilon_3 = \frac{-v_{31}}{E_1}\sigma_1 - \frac{v_{32}}{E_2}\sigma_2 - \frac{\sigma_3}{E_3} \end{cases} \tag{3}$$

Voormeeren [3] derived

$$\begin{cases} v_{21} = v_{31} = \frac{v_0}{E_0}E_1 \\ v_{12} = v_{32} = \frac{v_0}{E_0}E_2 \\ v_{13} = v_{23} = \frac{v_0}{E_0}E_3 \end{cases} \tag{4}$$

Substitution of (4) in (3) gives

$$\begin{cases} \varepsilon_1 = \frac{\sigma_1}{E_1} - \frac{v_0}{E_0}\sigma_2 - \frac{v_0}{E_0}\sigma_3 \\ \varepsilon_2 = \frac{-v_0}{E_0}\sigma_1 + \frac{\sigma_2}{E_2} - \frac{v_0}{E_0}\sigma_3 \\ \varepsilon_3 = \frac{-v_0}{E_0}\sigma_1 - \frac{v_0}{E_0}\sigma_2 - \frac{\sigma_3}{E_3} \end{cases} \tag{5}$$

From which the stiffness is solved

$$\begin{cases} E_1 = \frac{\sigma_1}{\varepsilon_1 + \frac{v_0}{E_0}\sigma_2 + \frac{v_0}{E_0}\sigma_3} \\ E_2 = \frac{\sigma_2}{\varepsilon_2 + \frac{v_0}{E_0}\sigma_1 + \frac{v_0}{E_0}\sigma_3} \\ E_3 = \frac{\sigma_3}{\varepsilon_3 + \frac{v_0}{E_0}\sigma_1 + \frac{v_0}{E_0}\sigma_2} \end{cases} \tag{6}$$

We define $\varepsilon_1' = \frac{\sigma_1}{E_1}$ etc., which be calculated as (according to Eq5)

$$\begin{cases} \varepsilon_1' = \varepsilon_1 + \frac{v_0}{E_0}\sigma_2 + \frac{v_0}{E_0}\sigma_3 \\ \varepsilon_2' = \varepsilon_2 + \frac{v_0}{E_0}\sigma_1 + \frac{v_0}{E_0}\sigma_3 \\ \varepsilon_3' = \varepsilon_3 + \frac{v_0}{E_0}\sigma_1 + \frac{v_0}{E_0}\sigma_2 \end{cases} \tag{7}$$

It can be seen that certain direction's Young's module depends on not only current direction's stress and strain but also other directions' as well as initial ratio of Young's module and Poisson ratio. Actually ε_1' and ε_3' are used for next section's damaged strength calculation.

If ε_1 would be used instead of ε_1', Young's modules can become negative on critical elements and the SLA process stops prematurely.

2.4 General formula for mapping back

Below are the equations for the intersection of two lines, derived with elementary mathematics.

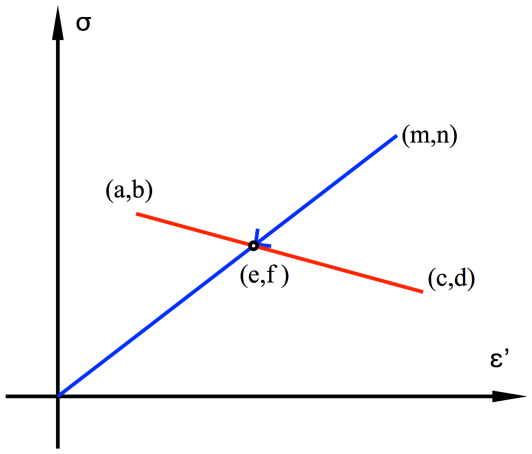

Figure 1: Elementary mathematics for calculating λ

$$e=\frac{(bc-ad)m}{(c-a)n-(d-b)m},\ f=\frac{(bc-ad)n}{(c-a)n-(d-b)m} \tag{8a}$$

$$\frac{n}{f} = \frac{c-a}{bc-ad}n - \frac{d-b}{bc-ad}m \tag{8b}$$

Coordinate (m, n) represents the computed strain and stress in a SLA step (too large). Line (a, b) - (c, d) represents the material failure curve. Intersection (e, f) represents the failure situation. Ratio $\frac{f}{n}$ represents the load factor λ.

The procedure for reducing the computed strain-stress to the failure strain-stress is called mapping back. Equation 8b is used in following calculation of λ.

For the Mohr-Coulomb criterion, there are two situations in compression, which are branch 1 and branch 2 (Figure 2). And for the tension criterion, there is only one softening branch to be considered.

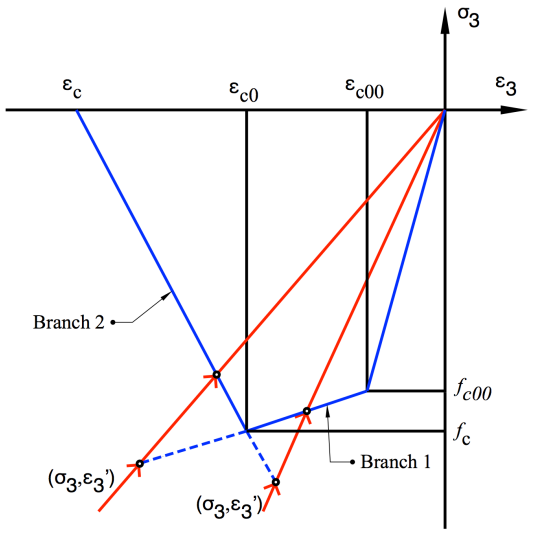

Figure 2: Calculations for compression part of the Mohr-Coulomb criterion

2.4.1 Mohr-Coulomb value for branch one

Below are the equations used to calculate Mohr-Coulomb value for branch 1.

When calculating $C_{M\text{-}C}$, Eq(1) and Eq (3b) are used.

$$c_1 = \frac{\varepsilon_{c0}-\varepsilon_{c00}}{f_{c00}\varepsilon_{c0}-f_c\varepsilon_{c00}} \quad (9)$$

$$c_2 = \frac{f_{c00}-f_c}{f_{c00}\varepsilon_{c0}-f_c\varepsilon_{c00}} \quad (10)$$

$$C_{c1} = \frac{\sigma_1}{f_{t2}} + c_1\sigma_3 + c_2\varepsilon_3' \quad (11)$$

where C_{c1} is 1/λ for branch 1.

2.4.2 Mohr-Coulomb value for branch two

Below are the equations used for calculating Mohr-Coulomb value for branch 2.

$$c_3 = \frac{\varepsilon_c-\varepsilon_{c0}}{f_c\varepsilon_c} \quad (12)$$

$$c_4 = \frac{f_c}{f_c\varepsilon_c} \quad (13)$$

$$C_{c2} = \frac{\sigma_1}{f_{t2}} + c_3\sigma_3 + c_4\varepsilon_3' \quad (14)$$

where C_{c2} is 1/λ for branch 2.

The largest 1/λ for branch 1 and branch 2 is the correct one,

$$C_{M\text{-}C}=\text{Max}\ (C_{c1}, C_{c2}) \quad (15)$$

2.4.3 Tension cutting-off value

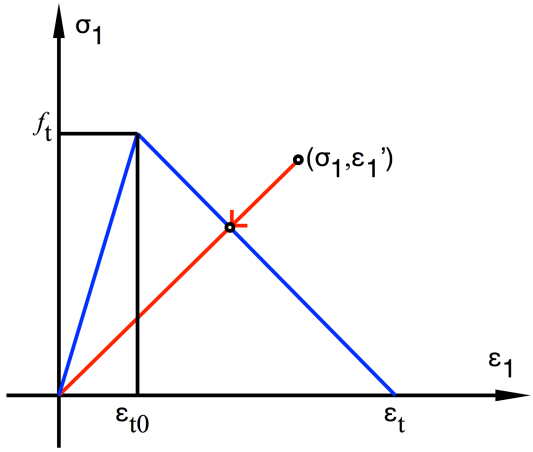

Figure 3: Calculations for tension cutting-off

There is only one situation (Figure 3), and the derivation is the same as above. But the difference is there is no compression part in C_t

$$t_1 = \frac{\varepsilon_t-\varepsilon_{t0}}{f_t\varepsilon_t} \quad (16)$$

$$t_2 = \frac{f_t}{f_t\varepsilon_t} \quad (17)$$

$$C_t = t_1\sigma_1 + t_2\varepsilon_1' \quad (18)$$

where C_t is tension cutting-off value $\sigma_1/f_t^{'}$.

The correct 1/λ is the largest of the Mohr-Coulomb value and the tension cutting-off value.

2.5 Orthotropic damage model and stiffness reduction

In the previous orthotropic model in SLA [3], as soon as the damage increments cause the principal stress to violate the tensile strength, a crack will be initiated perpendicular to the direction of the critical principal stress. After crack initiation in this critical integration point, the crack direction is fixed (fixed crack model). However, in the present new orthotropic model, every step's damage is in the principal direction of the critical element.

The damage direction changes along with the principal direction step by step (rotating crack model).

2.6 Calculation of constant-load factor *v*

In every SLA computation cycle, there is a linear relation between the force magnitudes and relevant stresses and strains.

This can be written as

$$F = \lambda_1(\frac{aF_c}{v_1} + bF_u) \tag{19}$$

where F is a force at some location of the structure and a and b represent the structure when F is equal to the local capacity that the correct λ is applied. The equation can be rewritten.

$$\frac{1}{\lambda_1} = \frac{1}{F}(\frac{aF_c}{v_1} + bF_u) \tag{20}$$

where $1/\lambda$ and $1/v$ have a linear relation (Figure 4). Just two calculation steps are sufficient to solve λ and v.

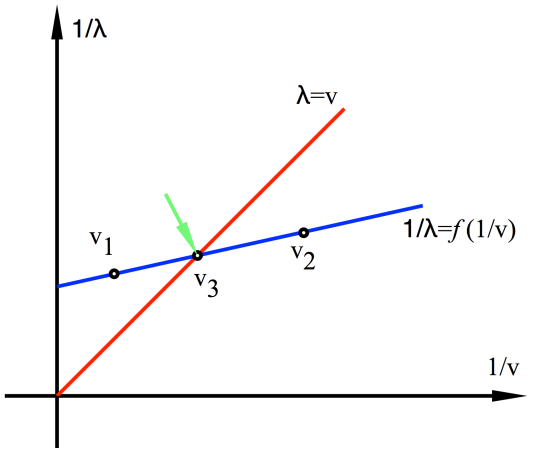

Figure 4: Function of constant load factor related to mapping back factor

The next step is similar, so

$$\frac{1}{\lambda_2} = \frac{1}{F}(\frac{aF_c}{v_2} + bF_u) \tag{21}$$

where a, b and F are not changed since Young's modules are not modified.

F_c will remain the same during mapping back step when

$$\lambda_3 = v_3$$

Therefore,

$$\frac{1}{\lambda_3} = \frac{1}{F}(\frac{aF_c}{v_3} + bF_u) \tag{22}$$

From Eqs. (20) (21) and (22), λ_3 and v_3 can be solved.

$$\lambda_3 = v_3 = \frac{-v_1\lambda_2v_2+\lambda_1\lambda_2v_2+\lambda_1v_1v_2-\lambda_1v_1\lambda_2}{v_1\lambda_2-\lambda_1v_2} \tag{23}$$

If it happens that λ_2 is almost equal to v_1, there is no need to sub-calculate λ_3. The condition for this is

$$|\frac{\lambda 2-v_1}{v_1}| \ll 1\% \tag{24}$$

For special situation when all forces are applied at the same position and in the same direction, below can the equation be simplified.

$$\frac{1}{\lambda_1} = \frac{a}{F}(\frac{F_c}{v_1} + F_u) \tag{25}$$

where F is real total failure force for this step. Therefore, one calculation step is needed to obtain λ and v.

$$\lambda_2 = v_2 = \frac{F_u\lambda_1v_1+F_c\lambda_1-F_cv_1}{F_uv_1} \tag{26}$$

2.7 Saw tooth model

The saw-tooth material model can make the fracture energy for SLA the same as for the physical non-linear analysis and it can also improve computational efficiency [4].

According to the research results of Rots [4], only an increase in strength for the saw tooth model would overestimate the peak load while only an increase in the ultimate strain would underestimate it. The best option is to increase both the strength as well as the ultimate strain of the saw tooth model.

The optimized saw tooth model for f_t = 1.43 MPa and ε_u = 0.002 is shown in Figure 5.

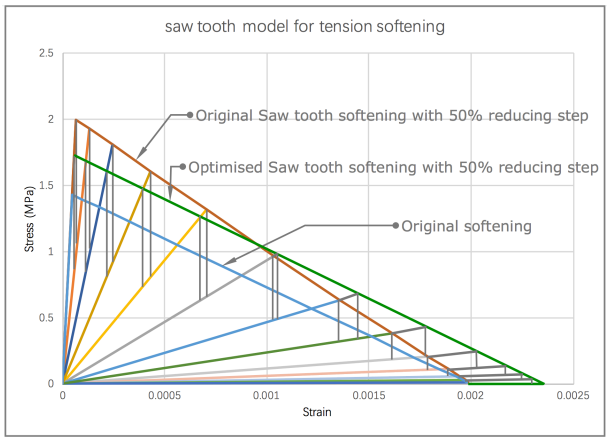

Figure 5: Optimized saw tooth model for tension softening compared with original one

3 TEST CASES

The experiment by Hordijk [5] is used for test, which is a simply supported concrete beam with two point loads at the top (Figure 6). The concrete element is plane183, the size of which is 5 mm.

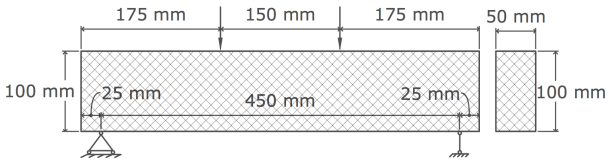

Figure 6: Test model dimension

Three load cases have been considered.

1) A vertical dead load D at the top. It is applied as two point loads of 1 kN.

2) A horizontal dead load H at both ends of the beam. It is also applied as a stress of 1 MPa over the total area of the beam ends.

3) A vertical live load L at the top. It is applied in the same way as load D. The magnitude of this load is increased to failure and reduced afterwards.

Two load combinations have been considered (Figure 7).

1) Dead load D + live load L (both in the same direction at the same location)

2) Dead load H + live load L (in different directions).



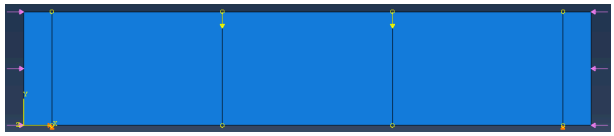

Figure 7: FEM model with load case D(top) and H(down)

3.1 Material properties and modified material model

This study considers softening for tension and compression. The concrete properties are E = 32000 MPa, Poisson's ratio = 0.2, tensile strength = 3 MPa, fracture energy = 0.06 N/mm. The compressive behaviour is elastic. Eq. 27 is used to determine ultimate strain for different element sizes (Figure 8).

$$G_{\mathrm{f}} = \frac{\varepsilon \sigma h}{2} \tag{27}$$

where h is the element size. The ANSYS model uses average stress which can be regarded as one integration point per element while the ABAQUS elements have four integration points per element. Therefore, the ultimate strain of the ANSYS models is halve of that of the ABAQUS model.

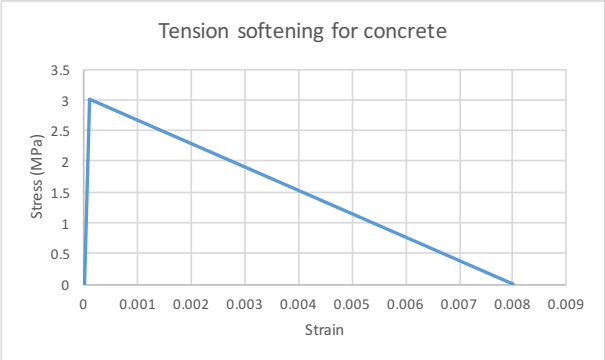

Figure 8: Material properties of concrete

Figure 9 shows the analysis steps when Young's modulus is sequentially reduced to 50% of the previous value. In the test cases reduction steps of 90% have been used. This has not been displayed here because it would produce an unclear picture.

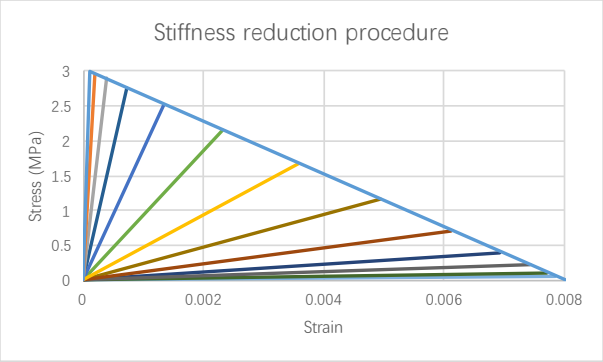

Figure 9: Sequentially reduced stiffness to 50% of the previous value

3.2 FEM model in ABAQUS and ANSYS

The analyses have been performed by SLA in ANSYS and by Newton-Raphson and arch length control in ABAQUS. The same material properties, element sizes and structural model have been used in ABAQUS and ANSYS (Figure 8). In ABAQUS the concrete damaged plasticity model is used to simulate concrete behaviour. This plasticity model is primarily intended to provide a general capability for the analysis of concrete structures under cyclic and/or dynamic loading. Under low confining pressures, concrete behaves in a brittle manner; the main failure mechanisms are cracking in tension and crushing in compression. The brittle behaviour of concrete disappears when the confining pressure is sufficiently large to prevent crack propagation. In these circumstances failure is driven by the consolidation and collapse of the concrete microporous microstructure, leading to a macroscopic response that resembles that of a ductile material with work hardening [6]. The parameters inputted for the concrete damaged plasticity model are: dilation angle is 30, eccentricity is 0.1, f_{b0}/f_{c0} is 1.16, K is 0.667, and viscosity parameter is 0.

The plane element used in ABAQUS is CPS8R, which is an 8-node biquadratic plane stress quadrilateral with reduced integration. The plane element used in ANSYS is PLANE183. It is a higher order 2-D, 8-node element. PLANE183 has quadratic displacement behaviour and is well suited for modelling irregular meshes. This element is defined by 8 nodes having two degrees of freedom at each node: translations in the nodal x and y directions. The element may be used as a plane element (plane stress, plane strain and generalized plane strain) or as an axisymmetric element. This element has plasticity, hyperelasticity, creep, stress stiffening, large deflection and large strain capabilities. It also has mixed formulation capability for simulating deformations of nearly incompressible elastoplastic materials and fully incompressible hyperelastic materials [7].

3.3 Analysis and comparison of the results

Two load combinations have been analysed. For combination one, two SLA analysis with different loads are compared. For combination two, SLA can only be compared with arc length analysis results.

3.3.1 Comparison of combination one

Two analyses have been performed. In the first analysis the beam is loaded just by force F_2 at the top which is increased until collapse. In the second analysis the beam is first loaded by force F_1 =1 kN at the top. Subsequently, the force F_2 is added to F_1 at the top. F_2 is increased until collapse.

The total force-displacement curves are almost identical (Figure 10) and the maximum error of total force is less than 1%.

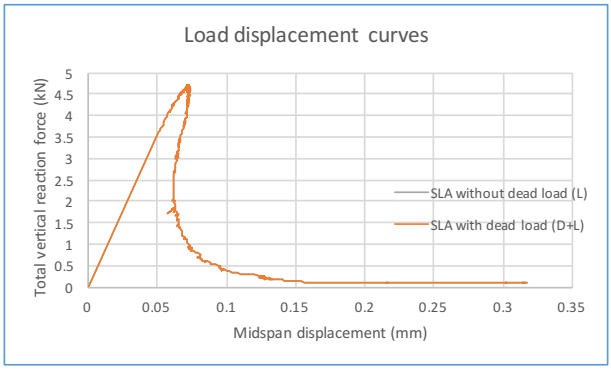

Figure 10: Dead load and point load are applied at the same position in the same direction. The curves are on top of each other.

3.3.2 Comparison of combination two

The horizontal pressure at the end of the beam is 1 MPa. The total reaction force is also a point load because the pressure is in the

horizontal direction. The SLA results fit well with ABAQUS non-linear analysis results (Figure 11). The differences mainly result from using average element results and saw tooth model's strength overshoot. The prestress is "constant" ranging from 0.99 to 1.01 MPa (Figure 12). And the constant load factors vary together with the mapping back factors, with almost the same values (Figure 13). Compared with the no prestress result in Figure 10, the prestress improves the structural stiffness and its capacity. It can be observed that the displacement is reduced for the same reaction force before the peak and the ultimate capacity increases from around 4.7 kN to 6.0 kN (Figure 14). This is caused by failure behaviour combined with bending and shear. In addition, prestress enhances the shear behaviour.

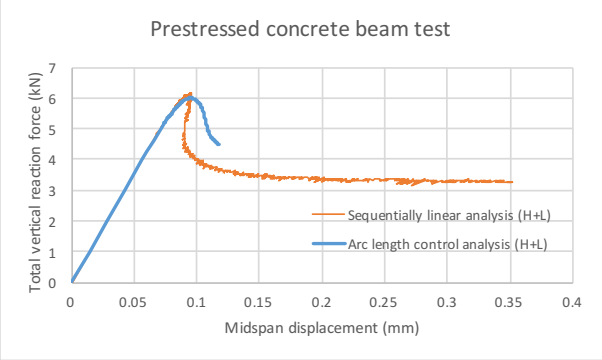

Figure 11: Load displacement curve comparison



Figure 12: Prestress-SLA step curve

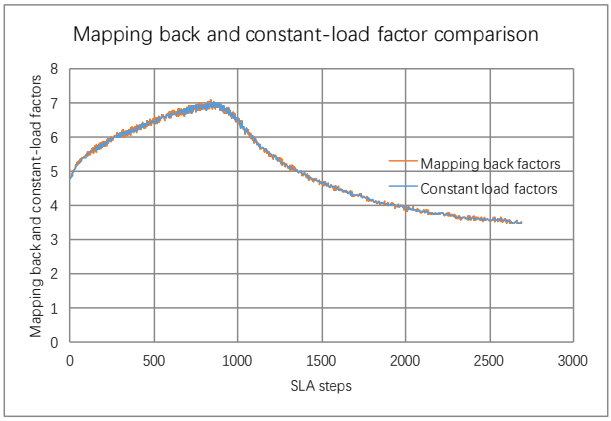

Figure 13: Constant load and mapping back factor comparison. The curves are overlapped.

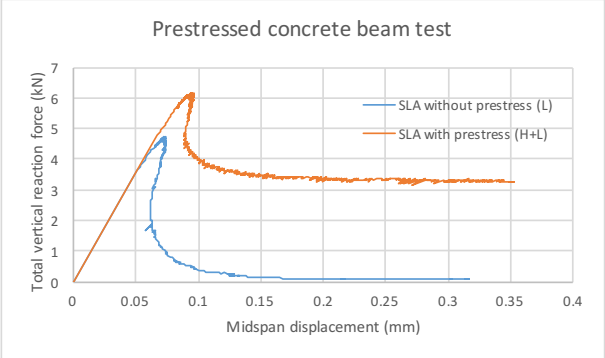

Figure 14: Prestress comparison for midspan point on RC beam test

The colour range of all principal strain contours below is defined in relation to the concrete's tensile softening behaviour values (Figure 15). From the principal strain contours (Figure 16), cracks concentrate around the middle of the beam. The structure meets the maximum capacity when cracks extend to the middle height of the beam and one element's maximum principal strain goes to the green zone. The two cracks are almost symmetric. However, after the peak, only the right-hand cracks continue developing. The reaction force plateau occurs in Figure 11 when the bottom part of the crack meets the ultimate strain. The crack patterns align well with arc length control results at the peak (Figure 17). Nevertheless, the arc length control cracks stay symmetric after the peak while SLA can localize one side of cracks, which is more realistic compared with the experiment. Because in reality there is no absolute symmetric structure and structures always have imperfections. Eventually cracks develop

to the top of the beam, which prevents the structure from carrying more load. Moreover, there is no compressive damage during the whole loading procedure, which also demonstrates that the orthotropic model works well. The damages develop basically only in *x* direction (Table 1).

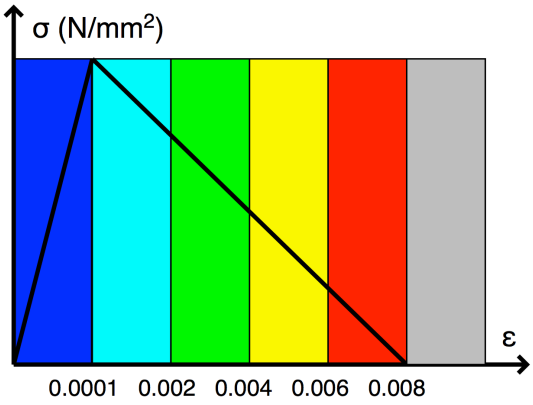

Figure 15: Colour range of principal strain contour

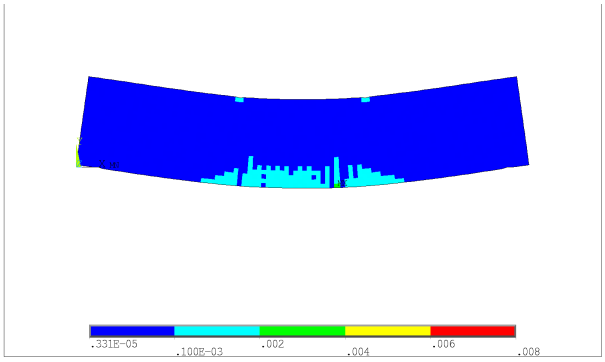

Figure 16a: Maximum principal strain at the peak by SLA

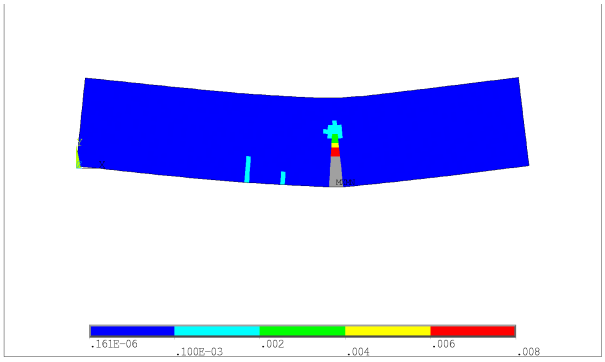

Figure 16b: Maximum principal strain after the peak by SLA

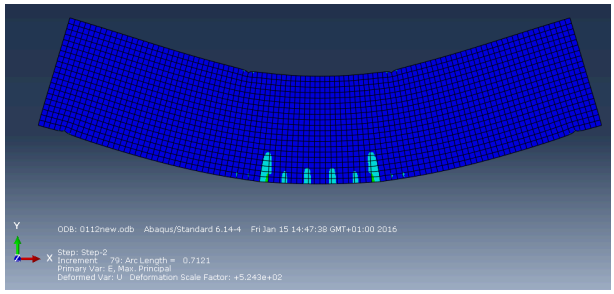

Figure 17a: Maximum principal strain at the peak by Arc length method

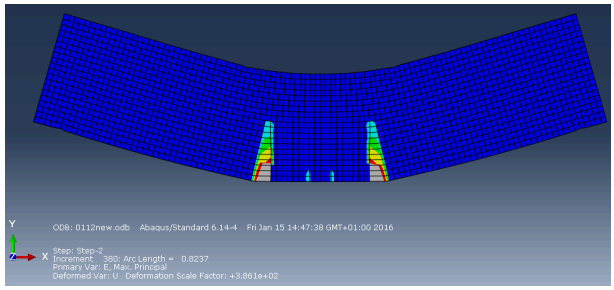

Figure 17b: Maximum principal strain after the peak by Arc length method

Table 1: An example of certain element stiffness reduction

Ex	*Ey*	*Ez*
32000	32000	32000
28800.001	32000	32000
28851.541	31999.714	32000
26018.092	31999.386	32000
23467.793	31999.005	32000
21166.375	31998.65	32000
19094.763	31998.222	32000
17224.998	31997.809	32000
15537.75	31997.4	32000
14019.009	31996.887	32000
12648.471	31996.36	32000
11411.927	31995.807	32000
10296.483	31995.212	32000
9290.454	31994.559	32000
8383.255	31993.826	32000
7565.312	31992.986	32000
6826.449	31992.151	32000
6160.586	31991.153	32000
5559.447	31990.104	32000
5016.936	31988.97	32000
4526.734	31987.863	32000

4084.211	31986.706	32000
3684.041	31985.682	32000
3322.575	31984.708	32000
2996.529	31983.658	32000
2703.5	31982.047	32000

4 CONCLUSION

The proposed algorithm for Sequentially Linear Analysis (SLA) of static non-proportional loading is simple, accurate, realistic and efficient. For non-proportional loading each SLA cycle can be determined in just two linear analyses. The algorithm can be applied to any element type (solid, plate, shell), failure criterion, load case (wind, snow, self-weight) and load combination.

Disadvantages of SLA are the considerable computation time and sensitivity to the size of stiffness decrements. The main advantage of SLA is its robustness; the algorithm always finds the correct load-displacement path. For example, it correctly predicts that just one crack will occur in an unreinforced beam while the Newton-Raphson method needs a notch or imperfection at the correct location to produce this result.

REFERENCES

[1] J.G. Rots, B. Belletti, S. Invernizzi, Robust modeling of RC structures with an ‘‘event-by-event’’ strategy. *Engineering Fracture Mechanics* 75 (2008) 590–614

[2] M.J. DeJong, M.A.N. Hendriks, J.G. Rots. Sequentially linear analysis of fracture under non-proportional loading. *Engineering Fracture Mechanics* 75 (2008) 5042–5056

[3] L.O. Voormeeren. Msc thesis- Extension and Verification of the Sequentially Linear Analysis to Three-Dimensional Cases. 7-12, Delft University of Technology, 2011

[4] J.G. Rots, S. Invernizzi. Regularized sequentially linear saw-tooth softening model. *International journal for numerical and analytical methods in geomechanics*, 28(2004) 821–856

[5] D.A. Hordijk, *Local approach to fatigue of concrete*, PhD Dissertation, Delft University of Technology, ISBN 90-9004519-8

[6] ABAQUS Theory Manual. 4.5.2 Damaged plasticity model for concrete and other quasi-brittle materials, ABAQUS software manual

[7] ANSYS software introduction, http://www.jlrcom.com/ansys-software.htm